Dynamics of xenon, krypton, and methane monolayers in registry with graphite

T. M. Hakim and H. R. Glyde
Department of Physics, University of Delaware, Newark, Delaware 19716

S. T. Chui
Bartol Research Institute, University of Delaware, Newark, Delaware 19716
(Received 23 July 1987)

The self-consistent phonon (SCP) theory is used to study the dynamics of monolayers of xenon, krypton, and methane adsorbed on graphite. Only the $\sqrt{3}\times\sqrt{3}$ solid phase is considered. It is shown that the phonon energies of the Xe monolayers are very similar to those of their floating counterparts, while the interaction of the Kr and CH_4 monolayers with the graphite significantly affects the phonon dispersion curves. The gap in the phonon dispersion curves at the center of the Brillouin zone is computed as a function of temperature. At a critical temperature, the gap goes spontaneously to zero and a transition from a locked-in commensurate phase to a floating phase takes place. This transition appears to describe the commensurate to floating transition in CH_4 well. A simple model of the floating transition is compared to the full SCP calculations. The one-phonon dynamic form factor, including the cubic anharmonic term, and phonon lifetimes are also evaluated for Kr and CH_4.

I. INTRODUCTION

The structure and dynamics of layers of atoms and simple molecules adsorbed on surfaces is a subject of great current interest. This interest is both to explore phase transitions and melting in two dimensions and to study phonons of 2D systems.[1-5] The purpose of the present paper is twofold. Firstly, we investigate the dynamics of solid monolayers of Kr, Xe, and CH_4 adsorbed on graphite. The aim is to evaluate the frequencies and lifetimes of in plane phonons in these two-dimensional (2D) solid films within the self-consistent phonon (SCP) theory. The dynamics of atoms and molecules in 2D solids have now been explored experimentally by neutron,[4,6,7] helium-atom,[8-10] and electron[11,12] beam scattering from adsorbed films. Particularly, neutron studies have determined powder averages of the phonon density of states of 2D ^{36}Ar films[6,7] adsorbed on graphite. These techniques hold great promise for detailed studies of phonons in 2D solids in the future. A specific goal is therefore to evaluate the one-phonon dynamic form factor $S_1(Q,\omega)$ for comparison with these experiments.

In an earlier paper[13] we evaluated the energies of phonons in an ideal, floating 2D solid (in the absence of a substrate) within the self-consistent harmonic (SCH) approximation. Here we incorporate the interaction between the 2D solid and the substrate, and add the cubic anharmonic term to the SCH dynamics so that phonon lifetimes can be obtained. Throughout, we assume that the monolayer is periodic so that the possibility of domain-wall formation is excluded.

Secondly, we explore the floating transition. At low temperatures we find the adsorbed monolayer is locked into a structure commensurate (C) with the substrate. There is a gap in the phonon-energy dispersion curves at the Brillouin-zone center (finite phonon energies at $q=0$). The root-mean-square (rms) vibrational amplitude $\langle u^2\rangle$ of the atoms vibrating around their equilibrium position is finite due to the interaction with the substrate. As the temperature is increased, the gap at the zone center closes and $\langle u^2\rangle$, which is determined simultaneously with the phonon energies in the SCP theory, increases. At a critical temperature ($T\approx 50$ K for CH_4 on graphite), the gap goes spontaneously to zero and simultaneously $\langle u^2\rangle$ diverges. The break in the translational symmetry induced by the substrate is lost, the monolayer floats above the substrate and translates freely. The floating transition has been discussed previously assuming a Debye-like phonon dispersion.[14] The gap equation is then analytically tractable and the floating transition temperature is found to depend on the square of the effective sound velocity. The present paper takes the full self-consistent phonon frequency into consideration. The gap equation is solved numerically, and it is seen that the floating transition temperature T_F is an order of magnitude less than that predicted by the simple model. In the full equations, T_F depends critically on the adatom-substrate interaction.

There is some evidence[15,16] of a transition from a locked-in, commensurate phase to a floating phase in CH_4 on graphite. The phase digram of CD_4 on graphite is shown in Fig. 1. For coverages $\rho\lesssim 1$ and at low temperatures, the CH_4 molecules are in the $\sqrt{3}\times\sqrt{3}R30°$ structure commensurate with the graphite (nearest-neighbor spacing 4.26 Å). At $T\approx 51$ K, Vora *et al.*[15] observed a transition to a "floating" phase in which the $\sqrt{3}\times\sqrt{3}$ structure remains but the nearest-neighbor

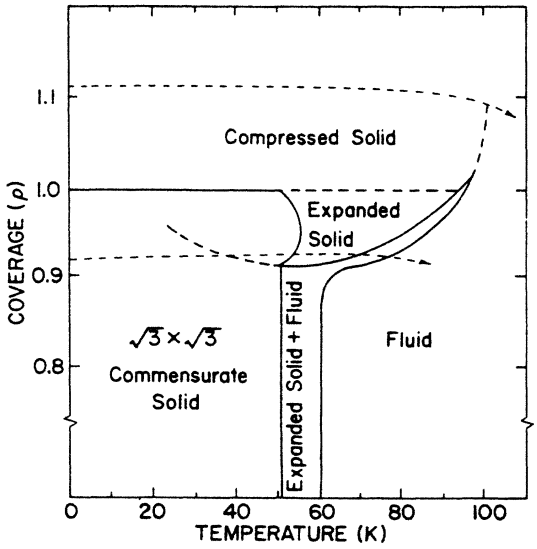

FIG. 1. Phase diagram of CD_4 on graphite from Ref. 16.

spacing expands as T is increased above 51 K. Glachant *et al.*[15] observed this transition to an expanded solid at $T=47-49$ K. There is no evidence[14,15] of domain walls in the expanded "floating" phase.

As the coverage ρ is increased above $\rho=1$, there is again a transition from a commensurate $\sqrt{3}\times\sqrt{3}R\,30°$ phase ($a=4.26$ Å) to a compressed $\sqrt{3}\times\sqrt{3}$ solid phase in which a is reduced below 4.26 Å (see Fig. 1). At low temperature, $T=5$ K and $1\leq\rho\leq1.1$, data analyzed by Dutta *et al.*[16] show the coexistence of two $\sqrt{3}\times\sqrt{3}$ solid phases; one having the commensurate spacing $a=4.26$ Å and another having a somewhat smaller spacing $a\approx4.20$ Å. At high temperature ($T=81.4$ K) and $\rho\gtrsim1$ the neutron data of Nielsen *et al.*[17] show only a single peak in the static structure factor characteristic of a single compressed $\sqrt{3}\times\sqrt{3}$ structure. There is no evidence of domain walls in the compressed phase in either case. Thus above a temperature of $T\approx50$ K, CH_4 molecules appear to float above the substrate in the $\sqrt{3}\times\sqrt{3}$ structure with its spacing free to expand or contract as thermodynamics dictates. The present calculation may therefore describe this commensurate to a floating transition well. Phillips[18] has previously predicted a floating phase for CH_4, using the quantum cell model. The latter is a single-particle model and it differs from our SCP theory in its circular averaging scheme, hence resembling the self-consistent Einstein technique. At all the temperatures of interest here, the CH_4 molecule may be regarded as freely rotating.

We have also investigated our simple model of a floating transition for parameters set to describe monolayers of Kr and Xe on graphite. The experimental situation is more complex in Kr. It has recently been reviewed by Abraham[5] and discussed in detail by Stephens *et al.*[19] and by Specht *et al.*[20] At $\rho\approx1$, adsorbed Kr is commensurate with the graphite. However, at high T, this commensurate phase melts directly into a fluid. There is no transition to an incommensurate phase at $\rho\approx1$. At $\rho>1$, Kr forms an incommensurate solid. At low T there is clear evidence of domain walls forming a honeycomb structure[5] in this incommensurate phase. At higher T ($T\approx100$ K) the walls are very mobile.[5] At high temperatures ($T\gtrsim95$ K) and for coverages $\rho>1$ far from the commensurate value ($\rho\approx1$), the data of Stephens *et al.*[19] shows no evidence of domain walls, and simulations[5] suggest rapidly mobile walls. In this region, the Kr could be reasonably described as floating and nearly periodic. As the coverage is increased,[20] the commensurate solid melts, then reenters into a narrow incommensurate solid phase. Koch and Abraham also found in computer simulation[21] that Kr undergoes an incommensurate to commensurate transition at $T\approx30$ K. This appears to result from the thermal expansion of the KR lattice spacing until it becomes commensurate[21] with the graphite value, $a=4.26$ Å.

In our calculation, we find that the floating temperature for Kr is 30 K. This seems too low and is very sensitive to the height of the modulation of the epitaxial-substrate interaction. We used a modulation parameter $V_G=-10$ K suggested by recent calculations[22,23] which is twice the modulation barrier proposed by Steele.[24]

In Xe, recent data of Venables *et al.*[25] confirm a commensurate phase over a narrow temperature range just below $T=60$ K which undergoes a transition to an incommensurate phase at $T=60$ K.

In Sec. II we describe our model of atoms adsorbed on graphite. The SCP theory is described in Sec. III. Phonon dispersion curves, phonon lifetimes and the one-phonon dynamic form factor, $S_1(Q,\omega)$, are presented in Sec. IV. The floating transition is discussed for CH_4, Kr, and Xe in Sec. V.

II. MODEL

On the exposed (002) face of graphite, the carbon atoms form a 2D honeycombed structure. Atoms such as Kr adsorbed on the (002) face have their lowest energy sited at the center of a hexagon. In the commensurate phase, the adsorbed atoms are locked into registry with the honeycomb structure and occupy every third hexagon center. This is referred to as the $\sqrt{3}\times\sqrt{3}R\,30°$ commensurate structure of adsorbed, solid monolayers. In it, the adsorbed atoms form an equilateral triangular lattice having nearest-neighbor distance $a=4.26$ Å.

A. Adatom-adatom potential

The adatom-adatom potential Φ_{AA} was assumed to be a sum of interactions between pairs only,

$$\Phi_{AA}=\tfrac{1}{2}\sum_{l,l'}v_A(\mathbf{r}_{ll'})\ .$$

For the Kr-Kr and Xe-Xe potential $v_A(r)$, we have used the Aziz-Chen form.[26] The specific parameters we employed are tabulated and explained in Ref. 13. Cardini and O'Shea[27] have found that the in-plane vibrations of commensurate Xe are insensitive to reasonable changes in the adatom-adatom potential.

At the temperatures of interest here, the CH_4 molecule adsorbed on graphite can be considered as freely rotating.[17] The CH_4-CH_4 interaction can then be reasonably approximated by a central potential depending only on the separation r between the molecules—as if they were atoms. In a detailed study, Righini *et al.*[28] have shown that this spherically averaged potential is very similar to the Kr-Kr interaction. We have therefore simply used the Aziz-Chen Kr-Kr $v(r)$ described above to represent the CH_4-CH_4 potential. This may oversimplify the interatomic potential, as we shall discuss below.

When the atoms are adsorbed on graphite, the latter responds like an elastic medium. To describe this a substrate mediated potential of the McLachlan form[29,30] was added to $v_A(r)$. It reduces the well depth of $v(r)$ by 10% to 20%.

B. Adatom-substrate potential

We denote by $B(\mathbf{r},z)$ the potential seen by an adsorbate atom due to its attraction by the graphite substrate. Here, z is the equilibrium height of the adatom above the substrate and $\mathbf{r}$ measures its location in the plane parallel to the graphite surface. The adatom has its minimum energy at a position immediately above a hexagon of the graphite lattice. Saddle points in the potential separate the minimum positions. The modulation of the $B(\mathbf{r},z)$ with $\mathbf{r}$ due to the graphite is usually expanded as a Fourier series with the height z taken as a parameter,[24]

$$B(\mathbf{r})=B_0(z)+\sum_{\mathbf{G}} B_{\mathbf{G}}(z)e^{i\mathbf{G}\cdot\mathbf{r}} .$$

From translational invariance, G's are reciprocal-lattice vectors $\mathbf{G}$ of the substrate.

The coefficients B are discussed in the literature.[31–34] We assume that the equilibrium height h of the adatoms above the substrate is independent of their location r on the substrate. The $B_0(z)$, which serves to determine the height h and is well known, then does not enter the dynamical equations. The modulation amplitudes $B_G(z)$ are not so well known. Since the B_G fall exponentially with increasing $|G|$, only terms corresponding to the first reciprocal shell S_1 are important. $B(r)$ in (1) is, then,

$$\begin{aligned} B(\mathbf{r}) &= \sum_{\mathbf{G}(\neq 0)} B_{\mathbf{G}}(h)e^{i\mathbf{G}\cdot\mathbf{r}} \\ &= 2V_G\left[\cos\left[\frac{4\pi}{b_0}x\right]+\cos\left[\frac{2\pi}{b_0}(x-y\sqrt{3})\right]\right. \\ &\quad \left.+\cos\left[\frac{2\pi}{b_0}(x+y\sqrt{3})\right]\right] , \end{aligned}$$

where $b_0=4.26$ Å and $\mathbf{r}=x\hat{\mathbf{i}}+y\hat{\mathbf{j}}$. Our $V_G\equiv B_G$ is half the value of V_G defined by Abraham.[5] We choose $V_G=-10$ K for krypton,[23] -6 K for xenon,[35] and -19.25 K for methane.[18] The adatom-surface potential can also be represented by a 12-6 Lennard-Jones interaction, but its weak variation across the basal plane makes the above truncation series computationally more convenient.[36]

III. SELF-CONSISTENT PHONON THEORY

The dynamics of the xenon, krypton, or methane monolayer adsorbed on graphite may be studied in a modified version of the self-consistent harmonic (SCH) model described in Ref. 13. An adatom at $\mathbf{r}_0$ is subjected to a potential which is the sum of the interparticle potential $\frac{1}{2}\sum_l v(\mathbf{r}_{0l})$ and the substrate potential $B(\mathbf{r}_0)$. The $v(\mathbf{r}_{0l})$ depends on relative separation $\mathbf{r}_{0l}$ while $B(\mathbf{r}_0)$ depends upon the position of the adatom relative to the substate.

The SCH equations may be derived by applying variational techniques[37] or any of the various approaches[38] followed in three dimensions. They differ from those describing the floating phase[13] in that there are now two essentially different terms, $v(\mathbf{r}_{0l})$ and $B(\mathbf{r}_0)$, in the total interaction.

The SCH frequency $\omega_{\mathbf{q}\lambda}$ of a phonon having a wave vector $\mathbf{q}$ and branch λ is given by

$$\omega^2_{\mathbf{q}\lambda}=\sum_{\alpha,\beta=1}^{2}\epsilon_\alpha(\mathbf{q},\lambda)\epsilon_\beta(\mathbf{q},\lambda)\frac{1}{M}\left[\left[\sum_l(1-e^{i\mathbf{q}\cdot\mathbf{R}_{0l}})\Phi_{\alpha\beta}(0,l)\right]+\Psi_{\alpha\beta}\right] , \tag{1}$$

where $\epsilon(\mathbf{q},\lambda)$ is the phonon polarization vector, M is the atomic mass, and $\mathbf{R}_{0l}$ define the Bravais lattice vectors.

The $\Phi_{\alpha\beta}$ are the force constants corresponding to $v(\mathbf{r}_{0l})$ averaged over $\mathbf{u}$, the relative vibrational amplitudes; $\mathbf{u}\equiv\mathbf{r}_{0l}-\mathbf{R}_{0l}$. They are given by

$$\begin{aligned} \Phi_{\alpha\beta}(0,l) &= \left\langle\frac{\partial^2 v(\mathbf{r}_{0l})}{\partial u_\alpha\,\partial u_\beta}\right\rangle \\ &= (2\pi^2|\overleftrightarrow{\Lambda}|)^{-1/2}\int d^2u\,\exp(-\tfrac{1}{2}\mathbf{u}\cdot\overleftrightarrow{\Lambda}^{-1}\cdot\mathbf{u}) \\ &\quad\times\frac{\partial^2 v(\mathbf{u}+\mathbf{R}_{0l})}{\partial u_\alpha\partial u_\beta} . \end{aligned} \tag{2}$$

The probability distribution is a Gaussian whose width is dictated by the relative displacement-displacement correlation $\overleftrightarrow{\Lambda}(0,l)$, such that

$$\begin{aligned} \Lambda_{\alpha\beta}(0,l) &= \langle u_\alpha(0,l)u_\beta(0,l)\rangle \\ &= \frac{\hbar}{MN}\sum_{\mathbf{q},\lambda}(1-e^{i\mathbf{q}\cdot\mathbf{R}_{0l}})\epsilon_\alpha(\mathbf{q},\lambda)\epsilon_\beta(\mathbf{q},\lambda) \\ &\quad\times\frac{\coth(\frac{1}{2}\beta\hbar\omega_{\mathbf{q}\lambda})}{\omega_{\mathbf{q}\lambda}} . \end{aligned} \tag{2'}$$

The $\Psi_{\alpha\beta}$ are the second derivatives of $B(\mathbf{r}_0)$ averaged over $\mathbf{w}$, the atomic displacements from equilibrium, $\mathbf{w}\equiv\mathbf{r}_0-\mathbf{R}_0$. Namely,

$$\Psi_{\alpha\beta}(l)=\left\langle \frac{\partial^2 B(\mathbf{r}_0)}{\partial w_\alpha \partial w_\beta}\right\rangle$$

$$=(2\pi^2|\xi|)^{-1/2}\int d^2w \exp(-\tfrac{1}{2}\mathbf{w}\cdot\overleftrightarrow{\xi}^{-1}\cdot\mathbf{w})$$

$$\times\frac{\partial^2 B(\mathbf{w}+\mathbf{R}_l)}{\partial w_\alpha \partial w_\beta}\ , \qquad (3)$$

and the displacement correlation matrix $\overleftrightarrow{\xi}(l)$ can be reduced to the following sum:

$$\xi_{\alpha\beta}(l)=\langle w_\alpha(l)w_\beta(l)\rangle$$

$$=\frac{\hbar}{2MN}\sum_{\mathbf{q},\lambda}\epsilon_\alpha(\mathbf{q},\lambda)\epsilon_\beta(\mathbf{q},\lambda)\frac{\coth(\frac{1}{2}\beta\hbar\omega_{\mathbf{q}\lambda})}{\omega_{\mathbf{q}\lambda}}\ . \qquad (3')$$

In (2') and (3'), $\beta=(k_B T)^{-1}$ and N is the number of atoms in the monolayer. Using $e^{i\mathbf{G}\cdot\mathbf{R}_l}=1$, Bloch's identity[39] for harmonic systems, $\langle e^{\hat{Q}}\rangle=e^{(1/2)\langle\hat{Q}^2\rangle}$, and the modulation expression for $B(r_0)$, $\Psi_{\alpha\beta}(l)$ becomes

$$\psi_{\alpha\beta}(l)=\left\langle \frac{\partial^2 B(l)}{\partial w_\alpha \partial w_\beta}\right\rangle$$

$$=-V_G\left\langle \sum_{G\in S_1} G_\alpha G_\beta \exp[i\mathbf{G}\cdot(\mathbf{R}_l+\mathbf{w}_l)]\right\rangle$$

$$=-V_G\sum_{G\in S_1} G_\alpha G_\beta \exp(-\tfrac{1}{2}\mathbf{G}\cdot\overleftrightarrow{\xi}\cdot\mathbf{G})\ . \qquad (3'')$$

Equations (1), (2), and (3) are from SCH theory. The quasiharmonic (QH) frequencies are obtained from (1) by taking the Gaussian vibrational distribution in (2) and (3) to be a δ function. The $\Phi_{\alpha\beta}$ and $\Psi_{\alpha\beta}$ reduce then to force constants evaluated with the atoms fixed at their sites $\mathbf{R}_l$. Starting with those QH frequencies, Eqs. (1), (2), and (3) are iterated until self-consistent to obtain the SCH frequency.

The SCH model takes into account only the even anharmonic terms to first order in the atomic interaction. These anharmonic terms are purely real, and therefore the phonons have infinite lifetimes. The cubic anharmonic term, in particular, is neglected. The cubic term is expected to be important and should be included in the study of anharmonic 2D systems to obtain a balanced theory, as was recently found for neon monolayers.[40] For example, while the even anharmonic terms increase the frequencies, the cubic term reduces the frequencies. With the cubic term included we may also readily evaluate the one-phonon dynamic form factor $S_1(\mathbf{q},\lambda;\omega)$. The lifetime of a phonon of a given branch λ and wave vector $\mathbf{q}$ is the inverse of the half width at half maximum (HWHM) of $S_1(\mathbf{q},\lambda;\omega)$. The cubic phonon energy is defined as the position of the maximum in $A(\mathbf{q},\lambda;\omega)$, the response function of the monolayer is an external disturbance of a given wave vector $\mathbf{q}$. This function, whose details are given elsewhere,[40] depends on the phonon energy shift $\Delta(\mathbf{q},\lambda;\omega)$ and inverse lifetime $\Gamma(\mathbf{q},\lambda;\omega)$. The relation between $A(\mathbf{q},\lambda;\omega)$ and $S_1(\mathbf{q},\lambda;\omega)$ is also presented in Ref. 40. The cubic anharmonic term is included in a model of floating Xe, Kr, and CH_4 monolayers to evaluate phonon lifetimes and response functions in monolayers for the first time.

IV. DISPERSION CURVES

The SCH phonon frequency dispersion curves for xenon on graphite at 0 K are displayed in Fig. 2 and compared with the results in which the Xe-substrate interaction is neglected. The interaction of the adsorbed atoms with the substrate is seen to introduce a gap in frequency at the center of the Brillouin zone ($q=0$). This means that the monolayer cannot undergo a zero-energy translation in the presence of a substrate. At $q=0$, the first term in (1) vanishes and

$$\omega_{0\lambda}^2=\frac{1}{M}\sum_{\alpha,\beta=1}^{2}\epsilon_\alpha(0,\lambda)\epsilon_\beta(0,\lambda)\Psi_{\alpha\beta}\equiv\Delta_G^2\ . \qquad (4)$$

The gap in the dispersion curves, Δ_G, depends only on $B(\mathbf{r},z)$ and not on the adatom-adatom interaction explicitly, as expected. For Xe, the gap at the zone center is 5.1 cm^{-1}, in good agreement with other calculations.[24,41] At other q values the phonon energies with and without a substrate differ at most by 4%. If the substrate-mediated interaction were ignored, the difference would be even smaller, but evidently the gap would not be affected.

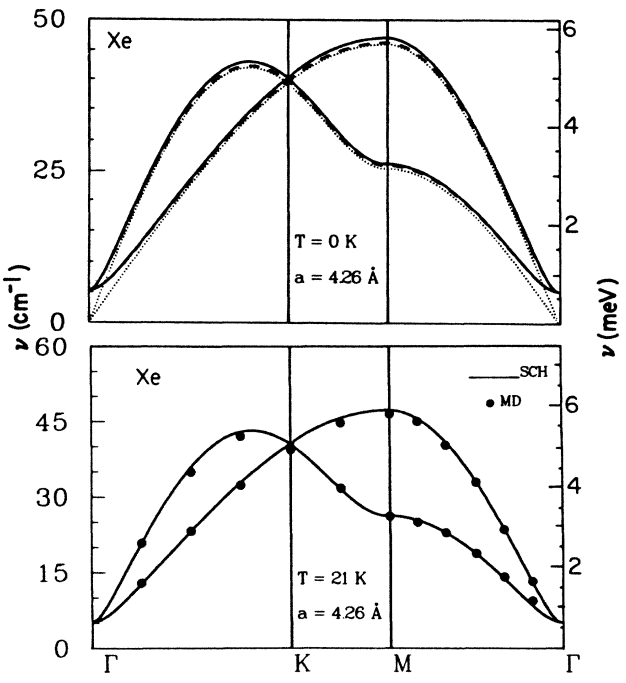

FIG. 2. Upper part: The SCH phonon frequency dispersion curves for xenon absorbed on graphite at 0 K along the $\Gamma KM\Gamma$ directions (solid curve). The dashed line is obtained with substrate mediation of the atom-atom interaction neglected. In the dotted curve all interaction of Kr with the substrate is neglected. Lower part: SCH dispersion curves for xenon compared with MD calculations (Ref. 41) at 21 K.

Also in Fig. 2, we compare the SCH results for Xe at 21 K with molecular-dynamics (MD) calculations.[41] The agreement is found to be better than one part in a hundred. The MD results also agreed well with the QH values.[41] This shows that anharmonic contributions, zero-point fluctuations, and the interaction of the substrate affect the phonon energies of Xe little, except at the zone center.

Unlike xenon, the physisorption of krypton on graphite affects its properties and the phonon energies significantly.[42–44] As shown in Fig. 3 the interaction with the substrate increases the phonon energies, from 10% to 20% between Γ and K. This difference decreases with increasing temperature, at fixed lattice spacing, but remains noticeable. The gap at $q=0$ is wider for krypton because the commensurate structure is more favored and the coefficient V_G is larger than for xenon. The volume dependence of the phonon energies is shown in Fig. 4. The krypton and xenon monolayers have to be expanded and compressed respectively to be in registry with the graphite structure, changing the stiffness drastically. This can be seen in the sound velocities in Table I. This difference in the stiffness leads to Grüneisen parameters which are larger in xenon than in krypton.[13] The Grüneisen parameters for Kr can be found from Fig. 4.

The SCH phonon energies for methane on graphite are shown in Fig. 5. The CH_4 phonon energies are almost three times larger than those for krypton. Since we used the same potential to describe the Kr-Kr interaction and the freely rotating CH_4-CH_4 molecule interaction, this difference is simply due to the difference in mass. The gap at Γ for CH_4 on graphite is also large, 25.8 cm^{-1} at 0 K and decreases slowly to 20 cm^{-1} at 40 K. The difference in gaps between CH_4 (25.8 cm^{-1}) and Kr (8.1 cm^{-1}) is due partly to the mass difference and partly to the difference in modulation height V_G: -19.25 K for CH_4 and -10 K for Kr.

We now include the contribution of the cubic anharmonic term to the dynamics of solid CH_4 and Kr monolayers. We consider only floating monolayers since the effects of interaction with the substrate have been investigated above. With the cubic anharmonic term included the phonon energies are shifted to lower values and the phonons have a finite lifetime. In Fig 6 we show the one-phonon dynamic form factor $S_1(Q,\omega)$ for Kr for a typical wave vector and $a=4.26$ Å. The phonon frequency is given by the position of the peak of $S_1(Q,\omega)$ and the inverse lifetime $\tau^{-1}=\Gamma$ by the half width at half maximum (HWHM) of the "one-phonon group."

In Fig. 7 we show the HWHM (τ^{-1}) and the peak position (ν) dispersion curves (solid lines) for phonons along the ΓK direction in Kr at 20 K. We see that the cubic anharmonic contribution reduces the phonon frequency (ν) typically by approximately 8% below the SCH values (dashed line). The anharmonic correction due to the even anharmonic terms contained in the SCH theory, given by the difference between the SCH (dashed) and QH (dotted) curves, is clearly larger than the cubic correction. The total anharmonic contributions, the SCH and the cubic term together, increase the phonon frequencies above the QH values by approximately 15% in Kr at 20 K. The HWHM dispersion curves (τ^{-1}) for the Kr monolayer are very similar to those found for bulk Kr with the longitudinal phonon having a maximum width about three-quarters of the way toward the Brillouin-zone edge. At the K point, the ratio ν/τ^{-1} is approximately 15, indicating that the phonon "oscillates" about 15 times before it decays. The

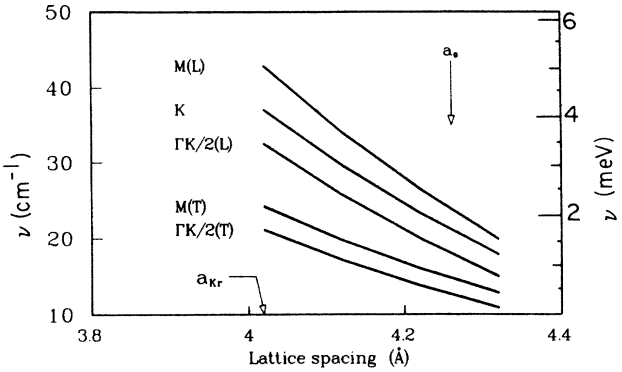

FIG. 4. Longitudinal and transverse phonon frequencies at special points in the Brillouin zone ($M,K,\Gamma,K/2$) as a function of lattice spacing for floating krypton monolayers; a_0 is the 4.26-Å graphite lattice spacing, a_{Kr} is the krypton equilibrium nearest-neighbor separation.

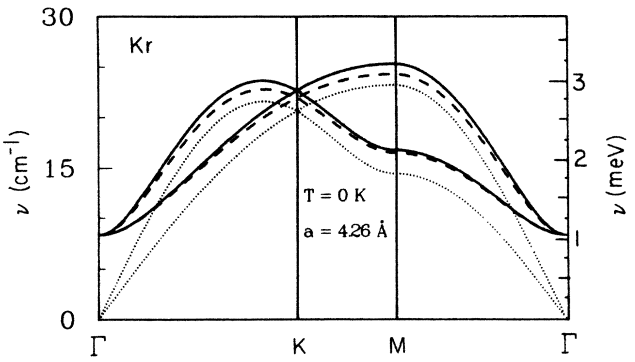

FIG. 3. The SCH frequency dispersion curves for krypton on graphite at 0 K, same legend as Fig. 2.

TABLE I. Transverse and longitudinal sound velocities in m/s of the $\sqrt{3}\times\sqrt{3}$ structure and at equilibrium lattice spacings for Xe and Kr at $T=0$ K.

	Xe		Kr	
	4.36 Å	4.26 Å	4.02 Å	4.26 Å
C_T	740	888	844	510
C_L	1284	1580	1465	790

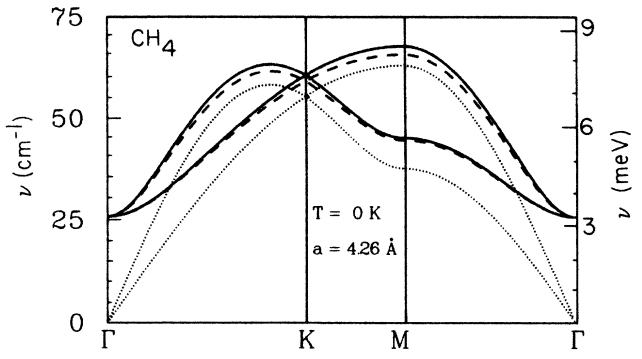

FIG. 5. SCH dispersion curves for methane at 0 K, legend as in Fig. 2.

phonons are therefore well defined with a sharp dynamic form factor as seen from Fig. 8.

The dynamic form factor $S_1(Q,\omega)$ for a floating CH_4 monolayer is shown in Fig. 9. Since we use the same interaction for CH_4 and Kr, the difference between CH_4 and Kr here is entirely due to the mass difference—a simple scaling. We see that $S_1(Q,\omega)$ is broader and CH_4 is more anharmonic due to the lighter mass. The cubic anharmonic term is relatively more important in CH_4—as reflected in the larger HWHM in Figs. 8 and 9 and in the larger cubic shift in the phonon frequencies shown in Fig. 9. The net increase in the phonon frequencies due to anharmonic terms above the QH values (difference between solid and dotted curves) is approximately 25–30% in CH_4. Thus anharmonic corrections are clearly very important in CH_4. They must be included in a realistic evaluation of the phonon dynamics.

V. VIBRATIONAL AMPLITUDES AND FLOATING TRANSITION

The other important effect of the substrate is that the gap at the zone center removes the logarithmic divergence of the mean-square vibrational amplitude $\langle u^2 \rangle$ at finite temperatures.[45] The $\langle u^2 \rangle$ is given by

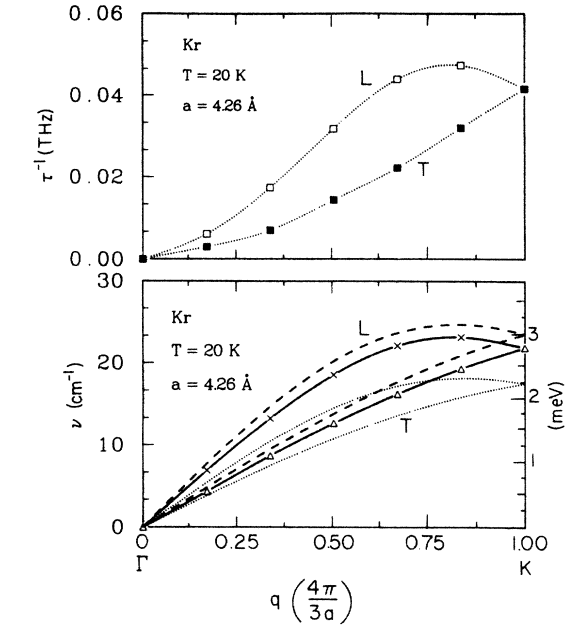

FIG. 7. Frequency (bottom) and inverse lifetime (top) dispersion curves for longitudinal (L) and transverse (T) phonons along ΓK in Kr. In the bottom figure the dotted curves are the QH values, the dashed are the SCH values, and the solid lines are the full phonon energies with the cubic term added.

$$\langle u^2 \rangle = \frac{\hbar}{2MN} \sum_{q,\lambda} \frac{\coth(\frac{1}{2}\beta\hbar\omega_{q\lambda})}{\omega_{q\lambda}} .$$

At $T=0$,

$$\langle u^2 \rangle = \frac{\hbar}{2MN} \sum_{q,\lambda} \frac{1}{\omega_{q\lambda}}$$

is finite for a 2D periodic lattice with or without the substrate. For $T>0$ K and in the floating case, $\langle u_{01}^2 \rangle^{1/2}$, the rms of the relative displacement between nearest neighbors and given by

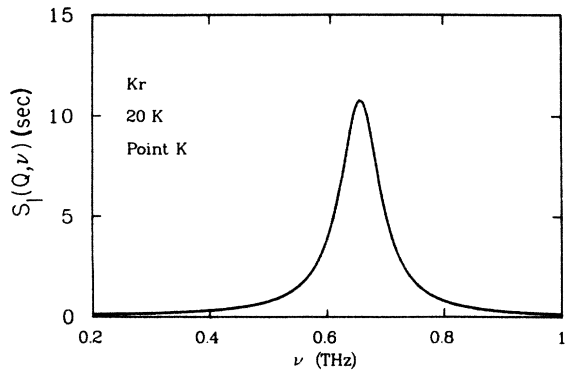

FIG. 6. $S_1(q,\omega)$ for Kr at point K (0.67, $2\pi/a$).

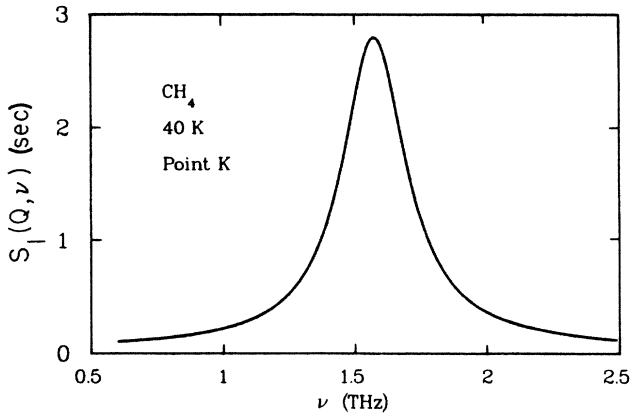

FIG. 8. $S_1(q,\omega)$ for CH_4 at point K.

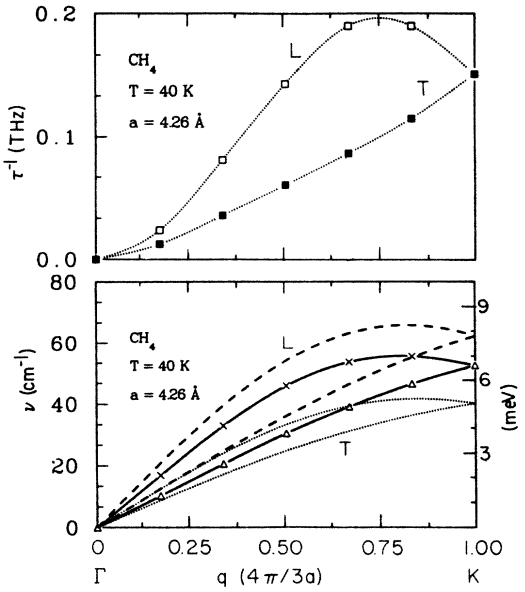

FIG. 9. Frequency and inverse lifetime dispersion curves for CH_4 along ΓK as defined in Fig. 7.

$$\langle u_{01}^2 \rangle = \mathrm{Tr}[\overleftrightarrow{A}(0)] = \sum_{q,\lambda} \frac{\hbar}{MN}(1-\cos \mathbf{q}\cdot\mathbf{R}_{01}) \times \frac{\coth(\frac{1}{2}\beta\hbar\omega_{q\lambda})}{\omega_{q\lambda}} ,$$

is also finite. This quantity works well as a replacement of $\langle u^2 \rangle$ in the consideration of Lindemann's ratio as a melting criterion.[46] We have previously[13] tabulated $\langle u_{01}^2 \rangle^{1/2}$ at three different temperatures for floating, infinite 2D solids.

The $\langle u_{01}^2 \rangle^{1/2}$ is also the quantity measured in the "Debye-Waller" factor of extended x-ray-absorption fine structure spectroscopy (EXAFS).[47] For Kr on graphite, our result for a commensurate structure, 0.19 Å, is in good agreement with the experimental number, (0.20±0.02) Å, at 10 K of Guryan *et al.*[47] In the floating case when the Kr-graphite interaction is neglected, this quantity becomes 0.28 Å.

In the presence of a substrate, the phonon frequency at small q can be approximated by a Debye-like expression:

$$\omega_{q\lambda}^2 \cong c_\lambda^2 q^2 + \Delta_G^2 , \quad (5)$$

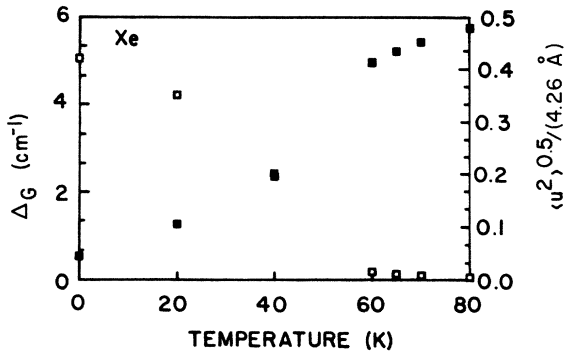

FIG. 10. The gap Δ_G and the Lindemann's ratio $\langle u^2 \rangle^{1/2}/4.26$ for xenon vs temperature: Open squares denote the gap (left-hand scale) while the solid squares denote Lindemann's ratio (right-hand scale).

where c_λ is an effective sound velocity of branch λ. Δ_G prevents $\langle u^2 \rangle$ from diverging. We tabulate the dimensionless rms displacement $\delta = \langle u^2 \rangle^{1/2}/a_0$ for xenon, krypton, and methane at several temperatures in Table II. The magnitude of δ depends critically on V_G as well as on the mass and force constants.

As the temperature is increased, the vibrational amplitude δ increases and the gap Δ_G decreases. At a critical temperature T_F, Δ_G becomes zero while δ becomes infinite and the monolayer "floats" above the substrate. The Δ_G and δ obtained in the SCH approximation are displayed as a function of T in Figs. 10–12. This floating transition and T_F are discussed below.

Since $\langle u^2 \rangle$ diverges logarithmically with sample size in the floating phase it is important to test whether our Δ_G and T_F are characteristic of the sample or simply size determined. To test this we show values of Δ_G as a function of the number of mesh points N in q space for Kr in Fig. 13. When N reaches 21 000 an asymptotic limit independent of N appears to be reached ($N = 20\,000$ corresponds to a sample size $L \approx 500$ Å). Increasing N further serves to lower T_F marginally. The values of Δ_G and $\langle u^2 \rangle$ shown in Figs. 10–12 are for $N = 21\,000$.

In Figs. 10–12, the SCH theory predicts a floating transition temperature of $T_F \approx 60$ K for Xe, 30 K for Kr, and 50 K for CH_4. At T_F, Δ_G vanishes and $\langle u^2 \rangle$ of our finite monolayers increases rapidly. In the floating phase, $\langle u^2 \rangle$ is infinite. It is finite here because we have

TABLE II. $\delta = \langle u^2 \rangle^{1/2}/a_0$, $a_0 = 4.26$ Å for Xe and Kr at several temperatures.

Kr		Xe		CH_4	
δ	T (K)	δ	T (K)	δ	T (K)
0.051	0	0.045	0	0.049	0
0.089	15	0.106	20	0.081	20
0.110	20	0.200	40	0.123	40
0.137	25			0.141	45

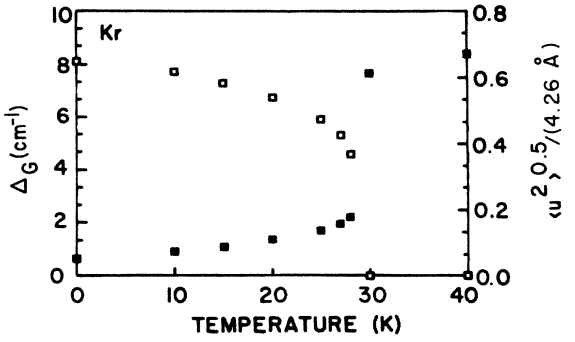

FIG. 11. Δ_G and Lindemann's ratio for krypton as in Fig. 11.

used a finite mesh size which corresponds to a finite sample size ($L \approx 500$ Å). As we mentioned earlier, this transition depends sensitively on the modulation of the substrate-adatom interaction and the mass of the adsorbate. This explains the high T_F for Xe in comparison to that of Kr and CH_4. The value of V_G is not precisely known for Kr; when we double it to -20 K, T_F moves up to 50 K. With this value of V_G, the only difference between Kr and CH_4, in our model, is their substrate screening potential and their masses. The latter produces a large difference in their zero-point energies E_z, and Debye temperatures,[13] $\Theta_D = 3E_z/2k_B = 35$ K for Kr versus 93 K for CH_4, both at $a = 4.26$ Å.

One can find an approximate analytic expression for T_F using a "Debye-like" model [Eq. (5)] for the phonon dispersion.[14] This gives (see the Appendix)

$$T_F = \left[\frac{NM}{Ak_B}\right]\frac{16\pi c^2}{G^2}, \tag{6}$$

where c^{-2} is the sum of the inverse square of the sound velocities in the floating phase, $G = 4\pi/4.26$ Å^{-1}, A is the area of the crystal, and M the atomic mass. This approximate T_F is not a function of V_G. If one uses the frequency around $q = 0$ to estimate c (Table I), this formula will provide a temperature equal to 640 K for Kr, which is larger by 1 order of magnitude than that obtained from our SCH calculation. Presumably, this

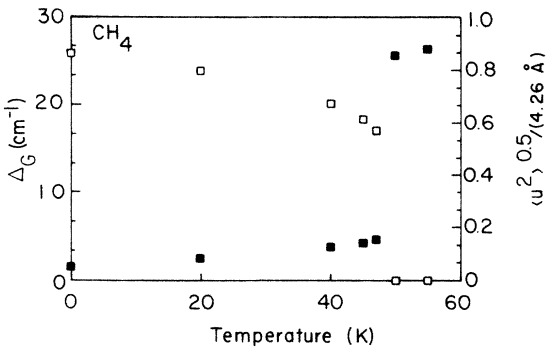

FIG. 12. Δ_G and Lindemann's ratio for methane as in Fig. 11.

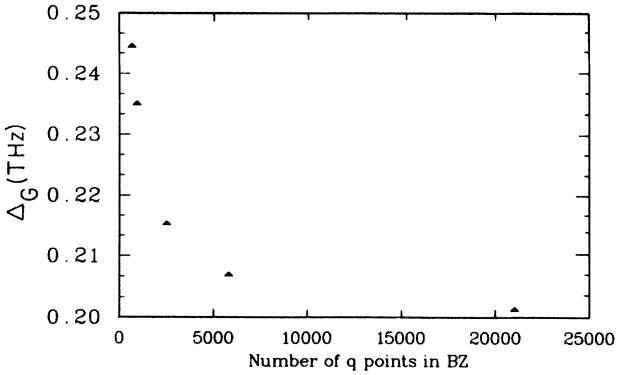

FIG. 13. The gap Δ_G for Kr dispersion curves at 20 K for several mesh sizes in the Brillouin zone.

comes from the sensitive dependence on the value of c used in Eq. (6). Indeed, if we pick c by dividing the zone-boundary phonon frequency by the zone-boundary wave vector, we obtain a transition temperature smaller than T_F by a factor of 8.

Including the dispersion in the phonon-frequency dispersion curves as well as the magnitude of V_G is important to obtain a reliable value of the floating transition temperature T_F.

VI. DISCUSSION

In the preceding section we saw that the monolayer undergoes a transition from a locked-in, commensurate phase at low temperature to a floating phase at high temperature. This transition occurs "naturally" within the SCH equations. At low T the atoms or molecules are locked into the commensurate position by the corrugation in the substrate potential. As T and the rms vibrational amplitude $\langle u^2 \rangle$ increase, the effect of the corrugation is smeared out until eventually the atoms float above the substrate. The transition temperature T_F depends sensitively on the barrier height of the corrugation determined by V_G. The SCH model predicts a $T_F = 50$ K for CH_4 on graphite which is very close to the observed[14,15] transition, $T_F = 48$–52 K. The present model restricts the monolayer to be periodic both above and below T_F. This appears to describe the observed transition in CH_4 well where no domain or domain wall structure is as yet observed in the floating phase.

The full SCH set of equations is qualitatively and quantitatively different from the simple Debye-like phonon dispersion model[2,14] given by (6) and discussed in the Appendix. The simple linear dispersion model does not depend explicitly on V_G and predicts a T_F a factor of 10 greater than the present SCH equations. Thus we believe it is important to take account of the dispersion and of V_G.

The present floating transition between periodic monolayers obtained within the SCH equations is far too restricted to describe the rich array of transitions observed in Kr. For Kr the present model predicts a floating transition at $T_F = 30$ K for[5] $V_G = -10$ K and

$T_F = 50$ K for $V_G = -20$ K. While this is in reasonable agreement with the observed transitions, neither domain-wall formation nor reentrant melting can be described. Also, since V_G is not well established, T_F is not certain in Kr. It is interesting to speculate why CH_4 and Kr behave so differently on graphite. This may be due to CH_4 being a molecule while Kr is an atom. The actual V_G for Kr may be higher than expected. If so, this can be determined experimentally from the gap in the phonon dispersion at the zone center. Also, quantum effects and therefore the light mass are more important in CH_4 above T_F. This may smear out effects of the substrate in the floating phase and prevent domain-wall formation. In CH_4, $T_F \sim \Theta_D/2$.

The critical nature of the floating transition is believed[2,3] to belong to the same universality class as the Kosterlitz-Thouless types. Our calculation does not determine the critical nature of the transition. However, we find the transition is sharp and takes place over quite a narrow temperature range of a few degrees in CH_4 and Kr. By contrast in Xe the transition in Fig. 10 has a width of the order of 20 K. We believe this large width is due to the small value of V_G and the large mass in the case of Xe. Since V_G is small the heavy Xe atom is not strongly localized, and with the large mass Xe responds "sluggishly" to increased temperature in the SCH equations. Otherwise the transition is sudden and the two phases do not coexist. Below T_F, $\langle u^2 \rangle$ in Table II depends largely on V_G. Above T_F, $\langle u^2 \rangle$ depends upon N (as $\ln N$) and is proportional to T. The present floating transition is very similar to SCH models of the ferroelectric or displacive transitions[48] and to models of mechanical instability[49] in crystals.

ACKNOWLEDGMENTS

It is a pleasure to acknowledge valuable discussions with Dr. B. Joos, Dr. A. D. Novaco, Dr. L. Passell, and Dr. H. Lauter. Support of the U. S. Department of Energy (Basic Energy Sciences Program) under Contract No. DE-FG02-84ER45082 is gratefully acknowledged.

APPENDIX

From (4) and the simplified expression for $\overleftrightarrow{\psi}(l)$ in (3''), we find

$$2\Delta_G^2 = \frac{B_1}{M} \sum_{\alpha,\beta} \sum_{\mathbf{G}\in S_1} G_\alpha G_\beta \exp(-\tfrac{1}{2}\mathbf{G}\cdot\langle \mathbf{uu}\rangle\cdot\mathbf{G}) , \tag{A1}$$

where in this appendix, $\mathbf{u} \equiv \mathbf{r}_0 - \mathbf{R}_0$ is the atomic displacement from equilibrium. In (3') we replace the sum by an integral to get

$$\langle u_\alpha u_\beta \rangle = \frac{\hbar}{2MN} \frac{A}{(2\pi)^2} \sum_{\lambda=T,L} \int d^2q \frac{\coth(\frac{1}{2}\beta\hbar\omega_{\mathbf{q}\lambda})}{\omega_{q\lambda}} \epsilon^\alpha_{\mathbf{q}\lambda}\epsilon^\beta_{\mathbf{q}\lambda} , \tag{A2}$$

where A is the area of the crystal. To evaluate (A2) we note the following: (i) for $T > \Theta_D$, where Θ_D is the Debye temperature,[13] $\coth(\frac{1}{2}\beta\hbar\omega_{\mathbf{q}\lambda}) \sim 2k_B T/\hbar\omega_{\mathbf{q}\lambda}$; (ii) $\omega^2_{\mathbf{q}\lambda} = (c_\lambda q)^2 + \Delta_G^2$ for $\lambda = T, L$ at small q [Δ_G is the gap (4) and c_λ are the sound velocities from the floating dispersion curves[13]]; (iii) $\epsilon_{qT}\cdot\hat{\mathbf{q}} = 1$ and $\epsilon_{qL}\cdot\hat{\mathbf{q}} = 0$; (iv) c_L and c_T are isotropic in the triangular symmetry, and

$$c^{-2} \equiv c_T^{-2} + c_L^{-2} = \frac{MN}{A} \frac{3\mu+\lambda}{\mu(2\mu+\lambda)} ,$$

where μ and λ are the corresponding elastic constants.

After evaluating the integral in (A2) using polar coordinates over a circle of large radius, we find the exponent in (A1) is

$$\tfrac{1}{2}\sum_{\alpha,\beta} G_\alpha G_\beta \langle u_\alpha u_\beta \rangle \simeq \left[\frac{kT}{2M}\right]\left[\frac{A}{N}\right]\left[\frac{G^2}{4\pi}\right] \times \sum_\lambda \frac{1}{c_\lambda^2} \ln\left[\frac{c_\lambda^2 q_D^2}{\Delta_G^2}\right] . \tag{A3}$$

The substitution of (A3) in (A1) yields

$$2\Delta_G^2 = -\frac{6\chi V_G}{M} e^{(2T\gamma \ln\Delta_G - xT)} , \tag{A4}$$

where

$$x = \frac{AG^2}{16\pi MN} \sum_\lambda \frac{1}{c_\lambda^2} \ln c_\lambda^2 q_D^2 ,$$

$$\gamma^{-1} = \left[\frac{16\pi}{k_B G^2}\right] \frac{\mu(2\mu+\lambda)}{3\mu+\lambda} , \tag{A5}$$

$$\chi = \sum_{\alpha=1}^{2} G_\alpha^2 .$$

Equation (A5) can be rewritten as

$$e^{-xT} \Delta_G^{2(T\gamma-1)} = -\frac{M}{3\chi V_G} . \tag{A6}$$

As temperature increases, the barrier of height V_G can no longer localize the atoms and at a critical temperature T_F, $\Delta_G \to 0$ and the atoms float above the substrate. At T_F the exponent of Δ_G must vanish so that

$$T_F = \gamma^{-1} . \tag{A7}$$

Equation (A7) is the analytic expression often used to determine T_F.

[1] J. M. Kosterlitz and D. J. Thouless, *Progress in Low Temperature Physics*, edited by D. F. Brewer (North-Holland, New York, 1978), Chap. 5, Vol. VII B; D. R. Nelson and B. I. Halperin, Phys. Rev. B **19**, 2457 (1979); A. D. Young, *ibid.* **19**, 1855 (1979); S. T. Chui, *ibid.* **23**, 5982 (1981).

[2] J. Villain, in *Ordering in Strongly Fluctuating Condensed Matter Systems*, edited by T. Riste (Plenum, New York, 1980), p. 221.

[3]*Ordering in Two Dimensions,* edited by S. K. Sinha (North-Holland, New York, 1980).
[4]S. K. Sinha, in *Methods of Experimental Physics,* edited by K. Sköld and D. L. Price (Academic, New York, 1986), Vol. 23, Pt. A.
[5]F. F. Abraham, Adv. Phys. **35**, 1 (1986).
[6]H. Taub, K. Carneiro, J. K. Kjems, L. Passell, and J. P. McTague, Phys. Rev. B **16**, 4551 (1977).
[7]C. Tiby and H. J. Lauter, Surf. Sci. **117**, 277 (1982).
[8]K. D. Gibson and S. J. Sibener, Phys. Rev. Lett. **55**, 1514 (1985); T. H. Ellis, G. Scoles, and U. Valbusa, Chem. Phys. Lett. **94**, 247 (1983).
[9]G. Brusdeylins, R. B. Doak, and J. P. Toennies, Phys. Rev. Lett. **44**, 1417 (1980); G. Brusdeylins, R. B. Doak, and J. P. Toennies, Phys. Rev. B **27**, 3662 (1983).
[10]J. P. Toennies, J. Vac. Sci. Technol. A **2**, 1055 (1984).
[11]S. Lehwald, J. M. Szeftel, H. Ibach, T. S. Rahman, and D. L. Mills, Phys. Rev. Lett. **50**, 518 (1983).
[12]J. M. Szeftel, S. Lehwald, H. Ibach, T. S. Rahman, J. E. Black, and D. L. Mills, Phys. Rev. Lett. **51**, 268 (1983).
[13]L. K. Moleko, B. Joos, T. M. Hakim, H. R. Glyde, and S. T. Chui, Phys. Rev. B **34**, 2815 (1986).
[14]B. I. Halperin and D. Nelson, Phys. Rev. Lett. **41**, 121 (1978); V. L. Pokrovsky and A. L. Talpov, *ibid.* **42**, 65 (1979). A similar result has been obtained earlier by Y. Saito in the context of the roughening transition.
[15]P. Vora, S. K. Sinha, and R. K. Crawford, Phys. Rev. Lett. **43**, 704 (1979); A. Glachant, J. P. Coulomb, M. Bienfait, P. Thorel, and C. Marti, *Ordering in Two Dimensions,* Ref. 3, p. 203.
[16]P. Dutta, S. K. Sinha, P. Vora, M. Nielsen, L. Passell, and M. Brek, *Ordering in Two Dimensions,* Ref. 3, p. 169.
[17]M. Nielsen, J. Als Nielsen, and J. P. McTague, *Ordering in Two Dimensions,* Ref. 3, p. 135.
[18]J. M. Phillips, Phys. Rev. B **29**, 5865 (1984).
[19]P. W. Stephens, P. A. Heiney, R. J. Birgeneau, P. M. Horn, D. E. Moncton, and G. S. Brown, Phys. Rev. B **29**, 3512 (1984).
[20]E. D. Specht, M. Sutton, R. J. Birgeneau, D. E. Moncton, and P. M. Horn, Phys. Rev. B **30**, 1589 (1984).
[21]S. W. Koch and F. F. Abraham, Phys. Rev. B **33**, 5884 (1986).
[22]G. Vidali, M. W. Cole, and J. R. Klein, Phys. Rev. B **28**, 3064 (1983).
[23]R. J. Gooding, B. Joos, and B. Bergerson, Phys. Rev. B **27**, 7669 (1983).
[24]W. A. Steele, Surf. Sci. **36**, 317 (1973).
[25]A. Q. D. Faisal, M. Hamichi, G. Raynerd, and J. A. Venables, Phys. Rev. B **34**, 7440 (1985).
[26]R. A. Aziz, *Interatomic Potentials for Rare Gases in Inert Gases,* edited by M. L. Klein (Springer-Verlag, New York, 1984), pp. 70–75.
[27]G. Cardini and S. F. O'Shea, Phys. Rev. B **30**, 7177 (1984).
[28]R. Righini, K. Maki, and M. L. Klein, Chem. Phys. Lett. **80**, 301 (1981).
[29]A. D. MacLachlan, Mol. Phys. **7**, 381 (1964); K. H. Lau, Solid State Commun. **28**, 757 (1978); L. W. Bruch and M. S. Wei, Surf. Sci. **100**, 481 (1980).
[30]S. Rauber, J. R. Klein, and M. W. Cole, Phys. Rev. B **27**, 1314 (1983).
[31]L. W. Bruch and H. Watanabe, Surf. Sci. **65**, 619 (1977).
[32]L. W. Bruch, Surf. Sci. **125**, 194 (1983). This paper reviews the physisorption interactions.
[33]M. W. Cole, D. R. Frankl, and D. L. Goodstein, Rev. Mod. Phys. **53**, 199 (1981); G. Vidali and M. W. Cole, Phys. Rev. B **29**, 6736 (1984).
[34]B. F. Mason and B. R. Williams, Phys. Rev. Lett. **46**, 1138 (1981).
[35]B. Joos, B. Bergerson, and M. L. Klein, Phys. Rev. B **28**, 7219 (1983).
[36]M. L. Klein, Y. Ozaki, and S. F. O'Shea, J. Phys. Chem. **88**, 1420 (1984).
[37]N. Boccara and S. Sarma, Phys. (N.Y.) **1**, 219 (1965); N. S. Gillis, N. R. Werthamer, and T. R. Koehler, Phys. Rev. **165**, 951 (1968).
[38]V. V. Goldman, G. K. Horton, and M. L. Klein, Phys. Lett. **28A**, 341 (1968); V. Samathyakanit and H. R. Glyde, J. Phys. C **6**, 1166 (1973); *Rare Gas Crystals,* edited by M. L. Klein and J. A. Venables (Academic, New York, 1976).
[39]S. Lovesey, *Theory of Neutron Scattering from Condensed Matter* (Oxford University Press, Oxford, 1984), p. 95.
[40]T. M. Hakim and H. R. Glyde, Phys. Rev. B (to be published), and references within.
[41]M. Marchese, G. Jacucci, and M. L. Klein, Surf. Sci. **145**, 364 (1984).
[42]N. D. Shrimpton, B. Bergerson, and B. Joos, Phys. Rev. B **29**, 6999 (1984).
[43]B. Joos and M. S. Duesbery, Phys. Rev. Lett. **55**, 1997 (1985).
[44]K. Kern, P. Zeppenfeld, R. David, and G. Cosma, Phys. Rev. B **35**, 886 (1987).
[45]B. Jancovici, Phys. Rev. Lett. **19**, 20 (1967); N. D. Mermin, Phys. Rev. **176**, 250 (1968).
[46]T. V. Ramakrishnan, Phys. Rev. Lett. **48**, 541 (1982).
[47]C. A. Guryan, K. B. Lee, P. W. Stephens, A. I. Goldman, J. Larese, P. A. Heiney, and E. Fontes (unpublished).
[48]N. S. Gillis and T. R. Koehler, Phys. Rev. B **5**, 1925 (1972); M. Cohen and T. L. Einstein, *ibid.* **7**, 1932 (1973).
[49]L. K. Moleko and H. R. Glyde, Phys. Rev. B **30**, 4215 (1984); L. L. Boyer, *Phase Transitions* (Gordon and Breach, London, 1985), Vol. 5, p. 1.